Nanoparticle Biodegradation

DOI: 10.1002/ange.201108280

Enzymatic Regioselection for the Synthesis and Biodegradation of Porphysome Nanovesicles**

*Jonathan F. Lovell, Cheng S. Jin, Elizabeth Huynh, Thomas D. MacDonald, Weiguo Cao, and Gang Zheng**

We recently reported that porphyrin–phospholipid conjugates can self-assemble into "porphysome" nanovesicles composed of a dense porphyrin bilayer.[1] Porphysomes exhibit structurally driven nanoscale optical properties and have intrinsic capabilities for multimodal imaging, drug delivery, and photothermal therapy. Previous studies were based on porphysomes formed from a mixture of two chemically similar phospholipid–porphyrin regioisomers. However, use of a mixture of regioisomers is far from ideal for robust nanoparticle characterization in vitro and in vivo. In general, difficulties in synthesizing, detecting, and distinguishing phospholipid regioisomers have prevented examination of their in vivo fate until now. To our knowledge, the results reported herein are the first to demonstrate in vivo enzymatic biodegradability for any intrinsically optically active nanoparticle, a feature that might be important when considering the use of new nanomaterials in human clinical trials.

Chemically modified phospholipids have proven useful for diverse biotechnology applications.[2–4] Phospholipids can be labeled at various positions on their head group or side chain.[5] While head-group modification can readily be achieved using the primary amine group of phosphatidylethanolamine, side-chain modification is less straightforward but is appropriate for conjugating more hydrophobic ligands while maintaining an amphipathic phospholipid character. Recently, phospholipids modified with cholesterol, retinoic acid, and porphyrin side chains have been developed that display useful properties for drug-delivery, immunological, and biophotonic applications.[1,6–9] Synthesis of single side-chain-modified phospholipids is often affected by acyl migration of the side chains. The resulting regioisomers (e.g., Figure 1a) have similar structures, which make their separation impractical and their detection challenging or impossible using techniques such as HPLC, NMR spectroscopy, and mass spectrometry.[10]

Regioselective phospholipid side-chain modification has been achieved using a number of techniques. Synthesis of modified phospholipids has been performed in multistep reactions using a modified glycerol backbone, with protecting groups sometimes being required.[6,9,11] Acylation of lyso-

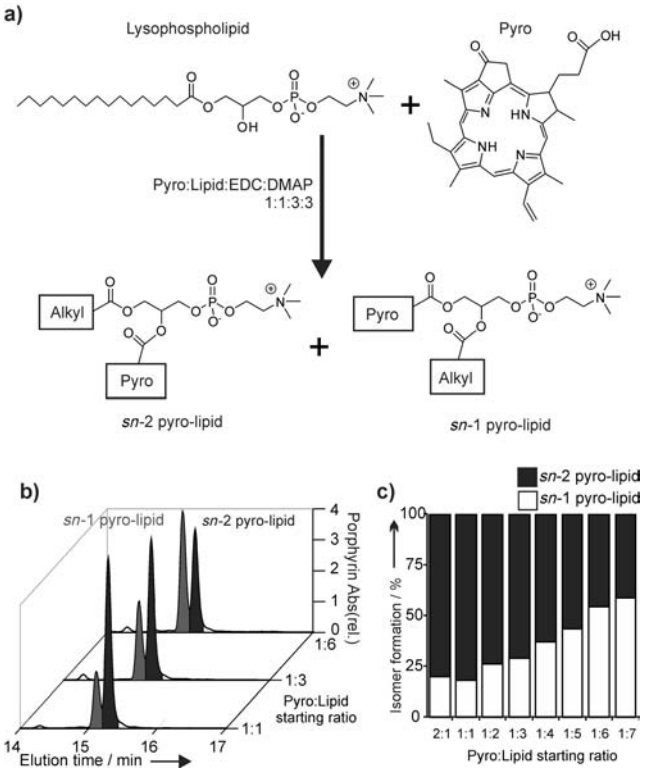

Figure 1. a) Synthesis of acyl-migrated pyro-lipid regioisomers. b) Detection of isomers by HPLC. c) Ratio of regioisomer products with respect to starting material ratios. EDC = *N*-ethyl-*N*′-[3-(dimethylamino)propyl]carbodiimide hydrochloride, DMAP = *N*,*N*-dimethylaminopyridine.

[*] J. F. Lovell, C. S. Jin, Prof. G. Zheng
Institute of Biomaterials and Biomedical Engineering
University of Toronto, Toronto, ON, M5G1L7 (Canada)
E-mail: gzheng@uhnres.utoronto.ca
Homepage: http://www.utoronto.ca/zhenglab
J. F. Lovell
Department of Biomedical Engineering, University at Buffalo
State University of New York, Buffalo, NY 14260 (USA)
C. S. Jin, T. D. MacDonald, Prof. G. Zheng
Department of Pharmaceutical Sciences, University of Toronto
Toronto, ON, M5G1L7 (Canada)
E. Huynh, Prof. G. Zheng
Department of Medical Biophysics, University of Toronto
Toronto, ON, M5G1L7 (Canada)
J. F. Lovell, C. S. Jin, E. Huynh, T. D. MacDonald, Prof. W. Cao, Prof. G. Zheng
Ontario Cancer Institute, the Campbell Family Institute for Cancer Research, and Techna Institute
University Health Network, Toronto, ON, M5G1L7 (Canada)
Prof. W. Cao
Department of Chemistry, Shanghai University
Shanghai (China)

[**] This work was supported by MaRS Innovation, the Canadian Cancer Society, CIHR, NSERC, and the Joey and Toby Tanenbaum/Brazilian Ball Chair in Prostate Cancer Research.

Supporting information for this article is available on the WWW under http://dx.doi.org/10.1002/anie.201108280.

phospholipids with fatty acid chlorides, imidazoles, anhydrides, and thiopyridyl esters has achieved varying degrees of isomeric purity (70–99%) and yield (40–90%), depending on the method and catalyst.[12,13] However, generation of these reactive intermediates may cause degradation and may not produce satisfactory yield or isomeric purity. Direct acylation of carboxylic acids to lysophospholipids with standard coupling agents is a convenient synthetic route, and protocols aiming to reduce acyl migration, such as sonication with glass beads, have been reported.[14] Herein, we develop a novel screen to identify enzymes that can be used in a scalable synthetic approach to generate either of the two regioisomers with excellent purity. Although porphysomes that were formed from either of the two regioisomers displayed similar physical properties, the biodegradability in vivo of the two regioisomers was strikingly different.

Pyropheophorbide-*a* (pyro) was attached to the lysophospholipid 1-palmitoyl-2-hydroxy-*sn*-glycero-3-phosphocholine in an acylation reaction using a pyro/lipid/DMAP/EDC molar ratio of 1:1:3:3. While this reaction proceeded to completion overnight, it generated two regioisomers, one with the pyro at the *sn*-2 position and one with the pyro at the *sn*-1 position, referred to as *sn*-2 pyro-lipid and *sn*-1 pyro-lipid, respectively (Figure 1a). The presence of the isomers was revealed by HPLC only when column heating to 60°C was used and two peaks eluted closely together (Figure 1b). Both these peaks demonstrated the same expected molecular weight and absorption spectra of pyro-conjugated phospholipid (Figure S1 in the Supporting Information).

The identity of the isomers was confirmed by examining the ^{1}H NMR chemical shift of the hydrogen on the central carbon atom of the glycerol backbone in the enzyme-cleaved conjugates, which was connected to either an ester or primary alcohol (enzymatic cleavage is described below and the NMR spectra of the cleavage products and the undigested regioisomers are shown in Figure S2 in the Supporting Information). Modulation of the starting ratios of pyro to phospholipid resulted in an altered ratio of the resulting regioisomer products. When a 2:1 pyro/lipid ratio was used, approximately 80% of the product was the *sn*-2 pyro-lipid isomer (i.e., pyro conjugated to the *sn*-2 hydroxyl group). When the ratio increased to 1:7, the *sn*-2 pyro isomer product decreased to 35% and the *sn*-1 pyro isomer increased to 65%. One explanation for this observation is that a small fraction of lysophospholipid underwent acyl migration prior to reaction with pyro. Since the acyl-migrated lysophospholipid contained a more reactive primary alcohol, it was rapidly consumed in the reaction so that a larger starting ratio of lysophospholipid resulted in the generation of more *sn*-1 pyro-lipid. Thus, some degree of regioisomer selection could be achieved by varying the reaction conditions, but an alternative approach was required to achieve improved isomeric purity.

Enzymes can be used to prepare or confirm the identity of phospholipids. For instance, phospholipase A2 may be used to cleave the substituent at the *sn*-2 position of phospholipids for the preparation of lysophospholipids or for analysis of cleavage products and side-chain properties. However, to our knowledge, enzymes have not yet been used synthetically to eliminate undesired phospholipid regioisomers. We hypothesized that the hydrophobic, planar character of pyro might interfere with enzyme recognition of the phospholipid conjugate in an isomer-specific manner. To test this hypothesis, a panel of 15 commercially available lipases and esterases was assembled and incubated with a near equimolar solution of *sn*-1 and *sn*-2 pyro-lipid. We did not optimize the reaction conditions or normalize enzyme activity units, as the purpose of the screen was to rapidly identify commercially available enzymes that could robustly cleave single regioisomers.

The isomeric cleavage of the various enzymes is shown in Figure 2a, with specific increase in *sn*-1 pyro-lipid shown in dark gray and specific increase in *sn*-2 pyro-lipid shown in light gray. Under the assay conditions, most enzymes were inefficient at cleaving the pyro-lipid regioisomers. This was not surprising, given the bulky steric interference introduced by pyro. However, some enzymes were identified that did act on pyro-lipid under the screening conditions. Esterase from *Bacillus stearothermophilus* efficiently cleaved both pyro-lipid regioisomers to a product with a mass-to-charge ratio of 848, which corresponds to pyro-lipid with the phosphocholine head group cleaved. However, no preferential cleavage of either regioisomer was detected. Several enzymes did selectively cleave *sn*-1 or *sn*-2 pyro-lipid regioisomers. Lipase from *Rhizomucor miehei* and *Pseudomonas cepacia* preferentially cleaved the *sn*-2 pyro-lipid isomer, although these enzymes cleaved substantial amounts of both isomers. Lipase from *Thermomyces lanuginosus* (LTL) selectively cleaved the *sn*-2 pyro-lipid regioisomer, with minimal modification of the *sn*-1 isomer. Conversely, phospholipase A2 from honey bee venom (PLA2HBV) selectively cleaved the *sn*-1 regioisomer. Reexamination of these two enzymes confirmed their specificity (Figure 2b). Thus, the screening approach identified two enzymes that could selectively cleave each regioisomer.

The *sn*-2 pyro-lipid synthetic route was more efficient not only since this avoided acyl migration (i.e., the conjugation took place on the lysophospholipid *sn*-2 alcohol as expected), but also because the optimized reaction did not require excess lysophospholipid (unlike the *sn*-1 pyro-lipid—see Figure 1c), which also minimized any risk of downstream lysophospholipid contamination. The synthesis of the *sn*-2 pyro-lipid could readily be increased to the 100 mg scale (Figure 2c) and consisted of three steps: conjugating the porphyrin to the lipid, digesting with enzyme, and purifying over a diol silica column. The isomeric purity plateaued at over 98% after a 10 h enzyme treatment (Figure S3 in the Supporting Information). This simple protocol was efficient and generated single-isomer *sn*-2 pyro-lipid with excellent purity. We subsequently scaled this reaction to the gram scale (data not shown). These *sn*-2 porphysomes were effective for photothermal therapy in which the synergistic effects of porphysomes and 1 min of laser irradiation at 671 nm (where porphysomes absorb) caused tumor heating to 60°C and permanent ablation of tumors in mice without any adverse side effects (Figure S4 in the Supporting Information).

Members of the phospholipase A2 family are known to cleave a variety of alkyl substituents at the *sn*-2 position, including fatty acid chains from two to greater than 20 carbon atoms.[15] Thus, it is likely that porphyrin is sufficiently

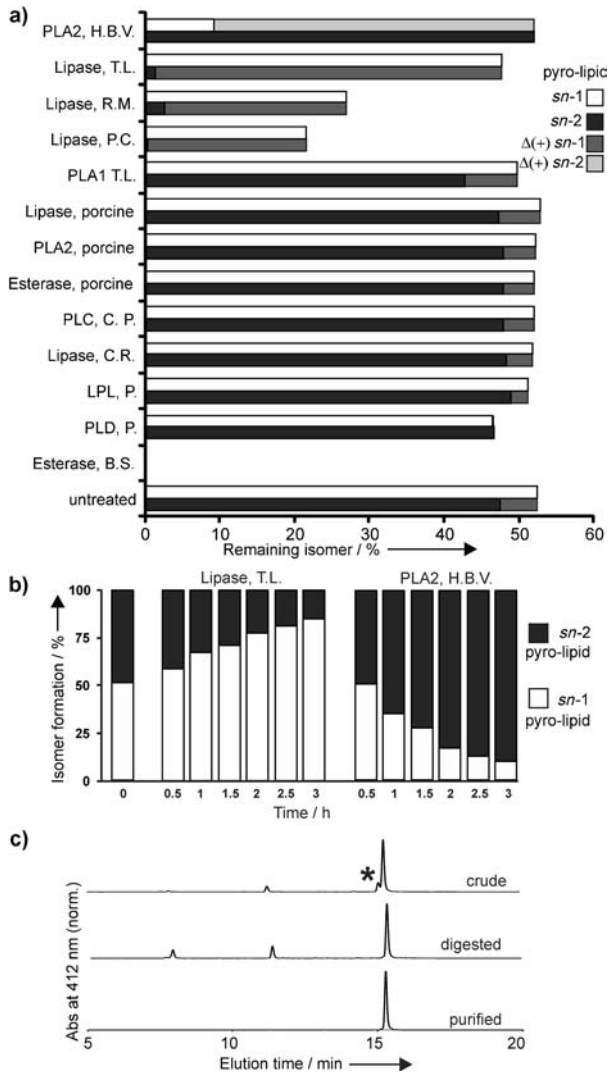

Figure 2. Identification of two enzymes that selectively cleave each pyro-lipid regioisomer. a) Isomer content following enzyme incubation of an *sn*-1 and *sn*-2 pyro-lipid solution. Abbreviations: PL: phospholipase; H.B.V.: honey bee venom; T.L: *Thermomyces lanuginosus*; R.M.: *Rhizomucor miehei*; P.C.: *Pseudomonas cepacia*; C.P.: *Clostridium perfringens*; C.R.: *Candida rugosa*; LPL, P: lipoprotein lipase, pseudomonas; PLD, P: phospholipase D, peanuts; B.S.: *Bacillus stearothermophilus*. The difference between the amounts of *sn*-2 and *sn*-1 isomers is shown in light gray and dark gray, respectively. b) Kinetic analysis of two hits identified in the enzyme screen capable of digesting each regioisomer. c) HPLC traces showing the enzymatic selection procedure at the 0.1 g scale using H.B.V. to produce pure *sn*-2 pyro-lipid. The asterisk indicates the *sn*-1 regioisomer.

different from an alkyl chain to interfere with enzyme recognition. It has also been observed that phospholipase A2 can cleave *sn*-2 alkyl side chains with various unnatural substituents at the *sn*-1 position.[16] These findings are consistent with the observation that PLA2HBV did not cleave the pyro located at the *sn*-2 position, but did cleave the alkyl chain when pyro was at the *sn*-1 position. Similarly, LTL is specific for alkyl side chains at the *sn*-1 and *sn*-3 positions, and for the same reason most likely does not recognize porphyrins at those positions.[17]

PLA2HBV and LTL were used for the preparation of isomerically pure pyro-lipid for assembly into porphysomes. The resulting *sn*-1 and *sn*-2 regioisomers were both over 97% isomerically pure based on HPLC. Each purified pyro-lipid regioisomer and a combination of the two, along with 5 mol% PEG-2000-phosphatidylethanolamine (PEG = polyethylene glycol) were prepared in a film, rehydrated, and extruded with a 100 nm membrane to form porphysomes. Transmission electron microscopy (TEM) confirmed the nanovesicle structure for porphysomes formed from each regioisomer, which comprised a spherical porphyrin bilayer encapsulating an aqueous interior (Figure 3, left column). Dynamic light scattering (DLS) showed that the size of the formulations in aqueous solution was monodisperse around 120 nm (Figure 3,

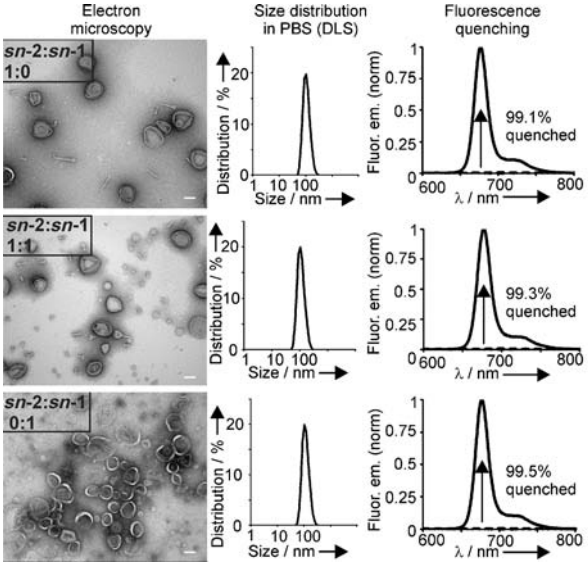

Figure 3. Both pyro-lipid regioisomers form porphysomes, which were produced with the indicated ratios of *sn*-2 or *sn*-1 pyro-lipid and subjected to TEM (left column). Scale bars: 100 nm. DLS is shown in the center column. Fluorescence spectra of the corresponding porphysomes are presented in the right column, with the spectra of the intact porphysomes shown as dashed lines and spectra after detergent disruption shown as solid lines. PBS = phosphate-buffered saline.

middle column). Another property of porphysomes comes from the face-to-face interaction of the pyro-lipid subunits within the porphyrin bilayer, which generates structurally driven self-quenching.[1] All porphysomes were highly quenched, with over 99% of the normal fluorescence emission of the pyro-lipid being quenched in the intact porphysomes (Figure 3, right column). Thus, both pyro-lipid regioisomers and a combination of the two behaved similarly in forming nanovesicles of highly quenched porphyrin bilayers.

Despite the chemical and physical similarities of the regioisomers and the nanovesicles self-assembled from them, they might be differentially metabolized, since the screen found that certain enzymes displayed regioselective behavior. The *sn*-1 and *sn*-2 regioisomers displayed similar single exponential half-lives in circulation (13.4 and 12.6 h, respec-

tively, Figure S5 in the Supporting Information). As shown in Figure 4a, 12 h after intravenous (I.V.) injection (750 nmol pyro-lipid per ca. 22 g mouse) the extracted mouse serum was notably colorful, as a result of the porphysomes that remained in circulation. In mice bearing subcutaneous xenografts, the biodistribution of both regioisomers in tumors was approximately 6–8% ID g^{-1} (ID = injected dose; Figure S6 in the Supporting Information) and both regioisomers could be directly visualized within cancer cells in a fixed tumor slice 24 h after I.V. administration (Figure S7 in the Supporting Information). The long circulation times of porphysomes allowed them to accumulate in tumors with high injected dose per gram, based on the enhanced permeability and retention effect.[18]

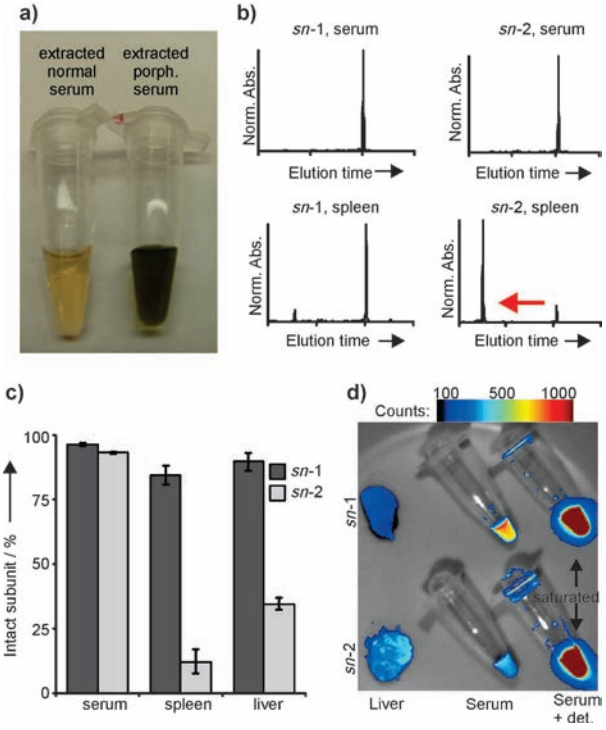

Figure 4. In vivo, regioselective biodegradation of porphysomes. a) Serum extracted from mice 12 h after I.V. injection of a therapeutic dose of porphysomes (ca. 750 nmol porphyrin–lipid). b) HPLC traces (abs. at 416 nm) of extracted serum or spleen. The elution time frame was from 5 to 20 min. The red arrow indicates pyro-lipid degradation product. c) Differential degradation of pyro-lipid in vivo; 12 h after I.V. administration, mouse organs and serum were extracted and integrity was quantified with HPLC. d) Pyro fluorescence in extracted organs and serum ±0.5% Triton X100 detergent. The signal was saturated in serum + detergent; further analysis showed the serum with detergent was 15–30 times brighter.

As pyro-lipid displayed strong absorption bands around 415 and 680 nm, HPLC traces could be readily obtained to verify the integrity of the starting material in vivo. In extracted serum, porphysomes formed from both *sn*-1 and *sn*-2 pyro-lipid remained chemically stable with minimal degradation products detectable by HPLC (Figure 4b). In the liver and spleen, organs that are central to the mononuclear phagocyte system in which PEGylated nanoparticles typically accumulate, the *sn*-1 porphysomes remained mostly intact. However, the *sn*-2 porphysomes underwent dramatic degradation. Nearly all the porphyrin–lipid was converted to a more hydrophilic degradation product, also suggesting that the degradation product could be porphyrin–phospholipid with the *sn*-1 alkyl side chain cleaved. Quantitatively, degradation was more efficient in the spleen than the liver for the *sn*-2 porphysomes (Figure 4c). Biodegradation was rapid, given the near complete degradation of the starting material even though some of the nondegraded porphysomes presumably accumulated in the liver and spleen throughout the course of the 12 h period. By examining the fluorescence of porphysomes in the liver, serum, and detergent-disrupted serum, it became apparent that despite the *sn*-2 pyro-lipid degradation, the affected nanoparticles maintained fluorescence self-quenching in the liver (Figure 4d). The fluorescence of the livers containing cleaved *sn*-2 porphysomes was only twofold brighter than those containing the intact *sn*-1 and pyro-lipid (assuming a similar biodistribution of porphysomes); however, the fluorescence change between serum with and without detergent disruption was 14- and 33-fold brighter, respectively (Figure S8 in the Supporting Information). Thus, the degraded *sn*-2 porphysome subunits appeared to maintain some fluorescence quenching in vivo.

In conclusion, two enzymes were identified in a screen (PLA2HBV and LTL) that could be used selectively for generating isomerically pure *sn*-1 and *sn*-2 porphyrin–lipid conjugates. The *sn*-2 pyro-lipid was effectively synthesized and could be used to ablate tumors using porphysome-mediated photothermal therapy. This enzymatic screening approach and the two enzymes identified here may be useful for generating other types of isomerically pure phospholipid conjugates. We demonstrated that regioisomeric phospholipid conjugates can generate nanoparticles that are physically similar, but vary greatly in how the nanoparticles biodegrade in vivo. Further research is warranted in studying the nature of enzymatic biodegradation of nanoparticles in vivo.

Received: November 24, 2011
Revised: December 15, 2011
Published online: January 20, 2012

Keywords: biodegradation · nanoparticles · phospholipids · porphyrinoids · regioselectivity

[1] J. F. Lovell, C. Jin, E. Huynh, H. Jin, C. Kim, J. Rubinstein, W. C. W. Chan, W. Cao, L. Wang, G. Zheng, *Nat. Mater.* **2011**, *10*, 324–332.
[2] R. W. Sinkeldam, N. J. Greco, Y. Tor, *Chem. Rev.* **2010**, *110*, 2579–2619.
[3] V. P. Torchilin, *Nat. Rev. Drug Discovery* **2005**, *4*, 145–160.
[4] A. Mueller, D. F. O'Brien, *Chem. Rev.* **2002**, *102*, 727–758.
[5] J. M. Rasmussen, A. Hermetter, *Prog. Lipid Res.* **2008**, *47*, 436–460.
[6] Z. Huang, F. C. Szoka, *J. Am. Chem. Soc.* **2008**, *130*, 15702–15712.
[7] Z. Huang, M. R. Jaafari, F. C. Szoka, *Angew. Chem.* **2009**, *121*, 4210–4213; *Angew. Chem. Int. Ed.* **2009**, *48*, 4146–4149.
[8] A. V. Popov, T. M. Mawn, S. Kim, G. Zheng, E. J. Delikatny, *Bioconjugate Chem.* **2010**, *21*, 1724–1727.

[9] D. S. Watson, Z. Huang, F. C. Szoka, *Immunol. Cell Biol.* **2009**, *87*, 630 – 633.
[10] A. Plueckthun, E. A. Dennis, *Biochemistry* **1982**, *21*, 1743 – 1750.
[11] O. Wichmann, C. Schultz, *Chem. Commun.* **2001**, 2500 – 2501.
[12] J. T. Mason, A. V. Broccoli, C.-H. Huang, *Anal. Biochem.* **1981**, *113*, 96 – 101.
[13] A. W. Nicholas, L. G. Khouri, J. C. Ellington, N. A. Porter, *Lipids* **1983**, *18*, 434 – 438.
[14] R. Rosseto, J. Hajdu, *Tetrahedron Lett.* **2005**, *46*, 2941 – 2944.
[15] D. A. Six, E. A. Dennis, *Biochim. Biophys. Acta Mol. Cell Biol. Lipids* **2000**, *1488*, 1 – 19.
[16] L. Linderoth, T. L. Andresen, K. Jørgensen, R. Madsen, G. H. Peters, *Biophys. J.* **2008**, *94*, 14 – 26.
[17] R. Fernandez-Lafuente, *J. Mol. Catal. B* **2010**, *62*, 197 – 212.
[18] J. Fang, H. Nakamura, H. Maeda, *Adv. Drug Delivery Rev.* **2011**, *63*, 136 – 151.

